American Mineralogist, Volume 77, pages 954–966, 1992

Activity-composition relationships in multicomponent amphiboles: An application of Darken's quadratic formalism

THOMAS M. WILL, ROGER POWELL
School of Earth Sciences, Department of Geology, The University of Melbourne, Parkville, Victoria 3052, Australia

ABSTRACT

Activity-composition (a-x) relationships in multicomponent amphibole solid solutions are modeled using Darken's quadratic formalism (DQF). In this, the thermodynamic behavior is expressed in terms of ideal mixing between real and fictive end-members, with the properties of the fictive end-members being constrained by the compositions of naturally coexisting amphibole pairs. The approach has been used to determine a-x relationships for calcic amphibole, sodic amphibole, cummingtonite, and orthoamphibole solid solutions in the system Na_2O-CaO-MgO-FeO-Al_2O_3-SiO_2-H_2O. This has been used to compare experimentally determined P-T-x conditions of formation of tremolite with those calculated by using our results. The correspondence is good and supports the application of DQF in modeling the activity-composition relationships in amphibole solid solutions.

INTRODUCTION

The modeling of mineral equilibria relies on two major sources of information: (1) thermodynamic data for mineral end-members and (2) the activity-composition (a-x) relationships of the end-members in minerals. In the last few decades thermochemical measurements and experimental phase equilibria studies have become more reliable and voluminous, and in particular, the thermodynamic properties of most of the main end-members of minerals are now relatively well determined (e.g., Holland and Powell, 1990). However, the a-x relationships of most complex minerals are still largely unknown; they are difficult to measure and would involve a phenomenal number of experiments to constrain, given that they are a function of composition as well as pressure and temperature. The absence of thermodynamic data becomes complete when considering the a-x relationships of mineral end-members that cannot be synthesized, for example, the tremolite end-member in the orthoamphibole structure. Pure tremolite cannot be made in the orthorhombic *Pnma* structure, so its properties cannot be measured nor can experiments be performed on its stability. In fact, experiments on stoichiometric tremolite are not possible because tremolite forms a solid solution with cummingtonite in the CaO-MgO-SiO_2-H_2O system. In this type of solution, not only are the a-x relationships for the end-members not known but also the end-member properties themselves. Given experimental or natural data on mineral equilibria, it is the Gibbs energy of an end-member, G_k, in combination with its activity in the form, RT ln a_k, that is constrained by these data, not the two contributions separately. In a situation in which neither is known and in the presence of limited a priori information, there is considerable latitude in the subdivision between G_k and RT ln a_k. This leads us to Darken's quadratic formalism, DQF, in which it is recognized that the formulation of a_k can be simplified dramatically for a particular choice of G_k (Powell, 1987).

Minerals of the amphibole group are stable under a wide range of P-T conditions in the Earth's crust and upper mantle. They are complex minerals and are subject to several substitutions: Tschermak's, $^{[4]}Al^{[6]}Al_{-1}(Fe,Mg)_{-1}Si_{-1}$, edenite, $Na^{[4]}Al\square_{-1}Si_{-1}$, and plagioclase, $Ca^{[4]}AlNa_{-1}Si_{-1}$, as well as $Ca(Fe,Mg)_{-1}$, $FeMg_{-1}$, and $Fe^{3+}Al_{-1}$. Because of the different charges and, in particular, sizes of the substituting cations, substitutions on the A and M4 sites cause miscibility gaps between the different amphiboles. Clearly, any thermodynamic model should be capable of describing these relationships. To complicate the determination of the thermodynamic parameters further, even though the thermodynamic properties for several amphibole end-members are now relatively well known (e.g., Holland and Powell, 1990), there are many end-members in amphiboles for which the problem alluded to above applies (e.g., the tremolite end-member in cummingtonite); yet these end-members are important constituents of the minerals. This problem must be surmounted if realistic mineral equilibria involving amphiboles are to be calculated. In this paper, we attempt to deduce a thermodynamic model for amphiboles from the compositions of coexisting amphiboles in rocks using DQF.

MULTICOMPONENT DQF

The modeling of a-x relationships for solid solutions may be undertaken using information from phase equilibria, including experimental data, and data gained from rocks. As noted above, such data can only be used to determine G_k and RT ln a_k in combination for mineral end-members that do not occur naturally or cannot be synthesized. This situation applies to many of the end-members of interest in amphiboles, either because the

0003–004X/92/0910–0954$02.00

appropriate end-member does not occur with that symmetry (e.g., the monoclinic $C2/m$ tremolite end-member in the orthorhombic *Pnma* structure) or because a substitution does not occur to a sufficient extent (e.g., edenite in orthoamphiboles or in cummingtonite-grunerite solutions). In addition, the body of phase equilibrium data is not large, given the complexity of the system involved. As a consequence, a simple method of treating the data is essential.

DQF provides a simple method of representing the thermodynamic properties of complex solid solutions and their associated a-x relationships (Powell, 1987). Darken (1967) made the physicochemically plausible suggestion that it is unlikely that, in general, one mixing model can be applied satisfactorily over the entire compositional range of a given system. Instead, a simple mixing model might well be applicable over certain ranges of composition (simple regions), whereas complex relationships apply for the intermediate compositions between the simple regions. In general, binary systems can be considered in terms of two simple regions, each including an end-member, connected by a transitional region. Activity-composition relationships in each simple region can then be considered in terms of mixing between the "real" end-member (i.e., an end-member in one simple region) and a "fictive" end-member (i.e., the end-member in the other simple region). The simple mixing model used for each simple region has been the regular model, with ideal mixing obviously representing a special case of this. If the regular model, or ideal mixing, applies over the entire compositional range of a system without a transitional region being present, then the system corresponds to one simple region without any transitional regions, this representing a limiting case of DQF.

Given a generalization of this approach to multicomponent systems, as discussed below, DQF is useful in treating the amphibole data not least because of the fictive end-member aspect of the thermodynamic description, as the thermodynamic data for many pure end-members are unknown. As also discussed below, the order-disorder relationships in amphiboles are likely to be very complex, so attempting to use a mixing model to cover a wide range of amphibole compositions is likely to be unsuccessful, whereas DQF gives some promise of being able to circumvent the complexities. Moreover, DQF turns out to be able to describe the available phase equilibrium data with relatively few adjustable parameters.

In the context of applying DQF to complex minerals like amphiboles, it is apposite to discuss the application of DQF to multicomponent systems as well as to discuss the features of the mixing relationships that make the use of DQF reasonable.

Extension of DQF into multicomponent systems

Extension of DQF into multicomponent systems is straightforward, as can be seen using the microscopic rationale for DQF, assuming the applicability of the regular model in the simple regions. In the nearest neighbor model, from which the regular model can be derived, the energy of a system is calculated as the sum of contributions from the energies of next nearest neighbor pairs, ϵ_{kl}. Properties of a solid solution depend only on the characteristic potentials, $\Delta\epsilon_{ij}$:

$$\Delta\epsilon_{ij} = 2\epsilon_{ij} - \epsilon_{ii} - \epsilon_{jj} \quad (\text{for } i, j = 1, 2, \ldots, n;\ i \neq j)$$

for an n component system. These potentials are those that would apply in the corresponding i-j binary systems. Thus, in the binary system, if $\Delta\epsilon_{ij}$ is positive there will be an ordering tendency and each atom tends to surround itself with atoms of the other kind (i.e., a tendency to form a superlattice or addition compounds at low temperatures). If $\Delta\epsilon_{ij}$ is negative, i-i and j-j neighbors are preferred and at lower temperatures the solid solution tends to unmix into i-rich and j-rich regions.

In the regular model, the $\Delta\epsilon_{ij}$ are independent of composition and the interaction parameter w_{ij} is equal to $\Delta\epsilon_{ij}$, whereas in the subregular model, the $\Delta\epsilon_{ij}$ are a linear function of composition. The former implies that the constituent ϵ_{kl} have the same composition dependence or, indeed, that they are each composition independent. The latter implies that the ϵ_{kl} are each a linear function of composition. This requires that the atomic environment of each site, the controlling factor on ϵ_{kl}, also changes linearly with composition. Given that the energetic environment of a site is controlled by the dominant occupants, it seems more likely that the $\Delta\epsilon_{ij}$ are composition independent in the vicinity of end-members corresponding to the dominant occupants, forming simple regions, and that the $\Delta\epsilon_{ij}$ only vary between the simple regions. This is DQF, with simple regions being regular mixtures between real and fictive end-members and with transitional regions occurring between the simple regions. If any $\Delta\epsilon_{ij}$ are not composition dependent, then simple regions can include several end-members and not just be a compositional region around one end-member.

Order-disorder in minerals and DQF

Amphiboles not only involve the simple $FeMg_{-1}$ substitution but also $(Mg,Fe)Ca_{-1}$ as well as coupled substitutions such as the Tschermak and edenite substitutions. These substitutions undoubtedly give rise to strong order-disorder effects in the amphibole lattice as a consequence of the size and charge differences of the cations involved. These effects are clearly composition dependent in that they are controlled by the extent of the responsible substitution or substitutions. As a consequence, the geometrical arrangements of nearest neighbors and their energetics, and therefore the mixing properties, will change across the system and in a largely unknown way. The effect of the size and charge differences involved in the substitutions may also be strong enough to promote unmixing as well as symmetry changes. In the case of the amphiboles, unmixing occurs, as summarized by Ghose (1981) and recently documented for the tremolite-hornblende solid solution by Smelik et al. (1991), in addition

to changes in symmetry, for example, the $C2/m \leftrightharpoons P2_1/m$ and the monoclinic to orthorhombic transition associated with the $(Mg,Fe)Ca_{-1}$ substitution.

DQF may be used on complex systems, for example, in the presence of order-disorder phenomena, as a way of approximately describing systems that would otherwise be too complicated to handle at all. For a solid solution involving, for example, (coupled) substitutions, simple regions would correspond to ranges of composition in which the order-disorder effects are not changing too rapidly, and transitional regions would correspond to ones in which they are. In each simple region, the regular model is used to represent order-disorder. Whereas the end-members in the simple region are "real" and correspond to the actual order-disorder relationships, the fictive end-members for this region are ones having order-disorder corresponding to the symmetry of the real end-member in the simple region but for which, in reality, the ordering would be quite different. In this way, DQF can be used to accommodate the changing order-disorder that accompanies the substitutions. Clearly, the choice of compositional range for the simple regions is critical in the successful application of DQF.

Amphibole simple regions

The extent of the simple regions might be expected to relate to the ease of the substitutions involved. In the case of a substitution involving similar cations, for example $FeMg_{-1}$, it might be expected that a simple region would extend over the whole range of the substitution. Indeed, for $FeMg_{-1}$ the simple region may well be expected to be ideal in this dimension. For substitutions involving dissimilar cations or those that are coupled, the extent of the simple regions might not be expected to be wide. Thus, considering actinolitic amphiboles, referred to as actinolite, a simple region might be expected to include both the tremolite and iron tremolite end-members but not to extend too far in the direction of any of the miscibility gaps, for example toward the blue amphiboles.

For each of the amphibole solid solutions, the simple regions are assumed to involve much of the usual range of compositions, at least initially. In each case, this range of composition only involves a few end-members; in the case of actinolite, these are just tremolite and iron tremolite. Therefore the actinolite simple region is taken to involve the real end-members tremolite and ferroactinolite (the Fe equivalent of tremolite) and the fictive end-members hornblende, pargasite, and edenite (and their Fe equivalents) as well as the end-members that are important constituents of the other amphibole solid solutions (e.g., cummingtonite, glaucophane, etc.). At first sight, having, for example, hornblende as a fictive end-member in actinolite seems to present difficulties. However the experimentally derived Gibbs energy data for hornblende are obtained from experimental mineral equilibria data involving tremolite-hornblende solid solutions, and, as long as the data extraction process uses the same mixing model, no problem arises. In other words, the thermodynamic data for hornblende produced by this extraction process will actually be fictive.

The same logic applies in the case of the other solid solutions. The cummingtonite simple region involves real cummingtonite, fictive aluminum cummingtonite, and grunerite (because grunerite and cummingtonite have different symmetries). The blue amphibole simple region is taken to involve real glaucophane and ferroglaucophane and fictive richterite. The orthoamphibole simple region is taken to involve real anthophyllite and iron anthophyllite and fictive aluminum anthophyllite.

Adopting these simple regions, the mineral equilibrium data for naturally coexisting cummingtonite-actinolite, anthophyllite-actinolite, and actinolite-glaucophane pairs will be examined to find the extent of nonideality (the size of the regular model w's) in the simple regions.

Amphibole mineral chemistry

To choose the most appropriate thermodynamic description of the amphibole mixing behavior in the simple regions, we examine the compositional variations of the amphiboles first. For this, the structural formula of the amphiboles is recalculated as described in the next section.

Recalculation of the amphibole structural formula

The compositions of coexisting amphiboles have been obtained from a survey of the literature. For the cummingtonite-actinolite series, a total of 67 coexisting pairs have been processed using published mineral analyses from Kisch and Warnaars (1969), Kisch (1969), Haslam and Walker (1971), Immega and Klein (1976), Das Gupta (1972), Brady (1974), Sampson and Fawcett (1977), James et al. (1978), Stephenson and Hensel (1979), Hawthorne and Griep (1980), and those summarized by Klein (1968). Data summarized by Klein (1968) were also used for the orthoamphibole-actinolite series. The majority of the data used for these two solid solutions comes from amphibolite facies terranes. For coexisting calcic and sodic amphiboles, 49 pairs from greenschist-blueschist and eclogite facies terranes have been used with data from Ernst et al. (1970), Himmelberg and Papike (1969), Ernst and Dal Piaz (1978), Triboulet (1978), Schliestedt (1986), Reynard and Ballèvre (1988), and those summarized by Klein (1969).

The analyses were recalculated on the basis of 23 O atoms using an amphibole recalculation program written in Mathematica (Wolfram, 1988). With reference to the small number of published wet chemical analyses, the amount of Fe^{3+} as a percentage of total Fe in the electron microprobe analyses was estimated as follows: for cummingtonite-actinolite and orthoamphibole-actinolite pairs 5 and 15% and for calcic-sodic amphibole pairs 15 and 20%, respectively. Even though this approach is not entirely satisfactory, the recalculation of Fe^{3+} on the basis of, for example, charge balance is even more unsatisfactory because full site occupancy has to be assumed and the substitution of O for the OH group is ignored. In

cummingtonite and orthoamphiboles all Na was allocated to the A site, whereas in calcic and sodic amphiboles, Na was allowed to enter the M4 site as well. For all end-members, mixing on sites was assumed (Table 1). For the estimation of the mixing parameters, pairs have been rejected if the total of the recalculated analysis (wet and containing Fe^{3+}) was smaller than 98.5% or larger than 101.5%. From the remaining good analyses the mole fractions of the end-members (Table 1), ln K_d, and the standard deviation on ln K_d, $\sigma(\ln K_d)$, have been calculated for each pair. The calculation of $\sigma(\ln K_d)$ is an error propagation problem and is described in Appendix 1. For the error propagation, large uncertainties have been assigned to the estimated amount of Fe^{3+} in the amphiboles.

TABLE 1. Mole fractions and *a-x* relationships in amphibole end-members

Anthophyllite (*Pnma*)	$\square Mg_2Mg_3Mg_2Si_4Si_4O_{22}(OH)_2$
a (anth) =	$x_{\square,A}x^2_{Mg,M4}x^3_{Mg,M13}x^2_{Mg,M2}x^4_{Si,T2}$
Aluminum anthophyllite (*Pnma*)	$\square Mg_2Mg_3(MgAl)(Si_3Al)Si_4O_{22}(OH)_2$
a (alath) =	$37.93x_{\square,A}x^2_{Mg,M4}x^3_{Mg,M13}x_{Mg,M2}x_{Al,M2}x^3_{Si,T2}x_{Al,T2}$
Magnesium cummingtonite ($P2_1/m$)	$\square Mg_2Mg_3Mg_2Si_4Si_4O_{22}(OH)_2$
a (cumm) =	$x_{\square,A}x^2_{Mg,M4}x^3_{Mg,M13}x^2_{Mg,M2}x^4_{Si,T2}$
Aluminum cummingtonite ($P2_1/m$)	$\square Mg_2Mg_3(MgAl)(Si_3Al)Si_4O_{22}(OH)_2$
a (alcu) =	$37.93x_{\square,A}x^2_{Mg,M4}x^3_{Mg,M13}x_{Mg,M2}x_{Al,M2}x^3_{Si,T2}x_{Al,T2}$
Grunerite (*C2/m*)	$\square Fe_2Fe_3Fe_2Si_4Si_4O_{22}(OH)_2$
a (gru) =	$x_{\square,A}x^2_{Fe,M4}x^3_{Fe,M13}x^2_{Fe,M2}x^4_{Si,T2}$
Tremolite (*C2/m*)	$\square Ca_2Mg_3Mg_2Si_4Si_4O_{22}(OH)_2$
a (tr) =	$x_{\square,A}x^2_{Ca,M4}x^3_{Mg,M13}x^2_{Mg,M2}x^4_{Si,T2}$
Iron tremolite (*C2/m*)	$\square Ca_2Fe_3Fe_2Si_4Si_4O_{22}(OH)_2$
a (ftr) =	$x_{\square,A}x^2_{Ca,M4}x^3_{Fe,M13}x^2_{Fe,M2}x^4_{Si,T2}$
Hornblende (*C2/m*)	$\square Ca_2Mg_3(MgAl)(Si_3Al)Si_4O_{22}(OH)_2$
a (hb) =	$37.93x_{\square,A}x^2_{Ca,M4}x^3_{Mg,M13}x_{Mg,M2}x_{Al,M2}x^3_{Si,T2}x_{Al,T2}$
Tschermakite (*C2/m*)	$\square Ca_2Mg_3(AlAl)(Si_2Al_2)Si_4O_{22}(OH)_2$
a (ts) =	$64x_{\square,A}x^2_{Ca,M4}x^3_{Mg,M13}x^2_{Al,M2}x^3_{Si,T2}x^2_{Al,T2}$
Iron hornblende (*C2/m*)	$\square Ca_2Fe_3(FeAl)(Si_3Al)Si_4O_{22}(OH)_2$
a (fhb) =	$37.93x_{\square,A}x^2_{Ca,M4}x^3_{Fe,M13}x_{Fe,M2}x_{Al,M2}x^3_{Si,T2}x_{Al,T2}$
Glaucophane (*C2/m*)	$\square Na_2Mg_3(AlAl)Si_4Si_4O_{22}(OH)_2$
a (gl) =	$x_{\square,A}x^2_{Na,M4}x^3_{Mg,M13}x^2_{Al,M2}x^4_{Si,T2}$
Edenite (*C2/m*)	$NaCa_2Mg_3Mg_2(Si_3Al)Si_4O_{22}(OH)_2$
a (ed) =	$9.48x_{Na,A}x^2_{Ca,M4}x^3_{Mg,M13}x^2_{Mg,M2}x^3_{Si,T2}x_{Al,T2}$
Pargasite (*C2/m*)	$NaCa_2Mg_3(MgAl)(Si_2Al_2)Si_4O_{22}(OH)_2$
a (parg) =	$64x_{Na,A}x^2_{Ca,M4}x^3_{Mg,M13}x_{Mg,M2}x_{Al,M2}x^2_{Si,T2}x^2_{Al,T2}$
Richterite (*C2/m*)	$Na(CaNa)Mg_3Mg_2Si_4Si_4O_{22}(OH)_2$
a (rich) =	$4x_{Na,A}x_{Ca,M4}x_{Na,M4}x^3_{Mg,M13}x^2_{Mg,M2}x^3_{Si,T2}x_{Al,T2}$

Note: The space groups are given in parentheses following the mineral name; □ denotes a vacancy. The general structural formula is $A(M4)_2(M13)_3(M2)_2(T2)_4(T1)_4O_{22}(OH)_2$.

Chemical trends

Figure 1 contains a series of diagrams showing the compositional variations of the analyzed cummingtonite-actinolite pairs. As evident from these diagrams, there is a wide miscibility gap between coexisting cummingtonite and actinolite. The compositional range of the natural actinolite extends from tremolite to hornblende and about halfway toward calcic edenite (Figs. 1a, 1c). As indicated by the electron microprobe analyses, the actinolite shows a range of Ca on M4 and displays continuous Tschermak and edenite substitutions in the compositional range of the minerals analyzed (Figs. 1a, 1c) as well as a limited substitution of Na and Mg for Ca on M4 (Figs. 1d, 1e). Cummingtonite shows a small but important substitution of Ca for (Fe,Mg) on the M4 site (Figs. 1b, 1e) and limited Tschermak's and edenite substitutions toward aluminum cummingtonite and edenite (Figs. 1a, 1c).

Because of the different sizes and charges of the substituting cations, the nonideality in amphiboles must depend on the M4, M2, and A site occupancies. To see if this is the case, we plot the distribution coefficient, K_d, for various equilibria between coexisting amphibole pairs against various site fractions, X_i. For the cummingtonite-actinolite series, we may write many equilibria of the form:

$$\mu_k^{\text{Cumm } P2_1/m} = \mu_k^{\text{Act } C2/m} \quad (1)$$

for example

$$\mu_{tr}^{\text{Cumm } P2_1/m} = \mu_{tr}^{\text{Act } C2/m}$$

where upper case labeling refers to the mineral and lower case labeling to the end-member. Distribution coefficients can be written for each such equilibrium:

$$K_{d(1)} = \frac{x_k^{\text{Act } C2/m}}{x_k^{\text{Cumm } P2_1/m}}$$

in which x_k^j is the thermodynamic mole fraction of end-member k in phase j.

For a given equilibrium, for systems more complex than a binary, the slope of correlations on plots of ln K_d against site fractions are a linear combination of nonideal terms, each involving an interaction parameter, reflecting the energetic interactions between the various atoms on the various sites. For example, for coexisting cummingtonite-actinolite pairs, the contribution to nonideal mixing from interactions on M4 depends on interactions between Ca, Mg, and Fe and therefore involves terms involving $W_{MgFe,M4}$, $W_{MgCa,M4}$, and $W_{CaFe,M4}$. Horizontal trends correspond to ideal mixing between the real and fictive end-members.

Using the logic given above, we expect strong correlations between ln K_d and the M4, M2, and A site fractions, reflecting the nonideal character of the amphiboles and giving a measure of the nonideality involving these sites. For the equilibria given in Equation 1, Figure 2 shows a series of ln K_d vs. X_i diagrams. The error bars are 2σ, they were calculated using the error propagation outlined in Appendix 1. Within analytical error, the dependence of ln K_d on the M4, M2, and A site fractions can be described and fitted well by horizontal lines. This implies that the data obtained from the naturally coexisting amphibole pairs are consistent with and support zero interaction parameters. Therefore, in the simple regions, the amphibole mixing behavior can be adequately described by ideal mixing between the real and fictive end-members.

Given the complexity of the substitutions involved, the fact that the data are consistent with an ideal mixing description in the simple regions is surprising. From a microscopic point of view, this is unlikely to be warranted

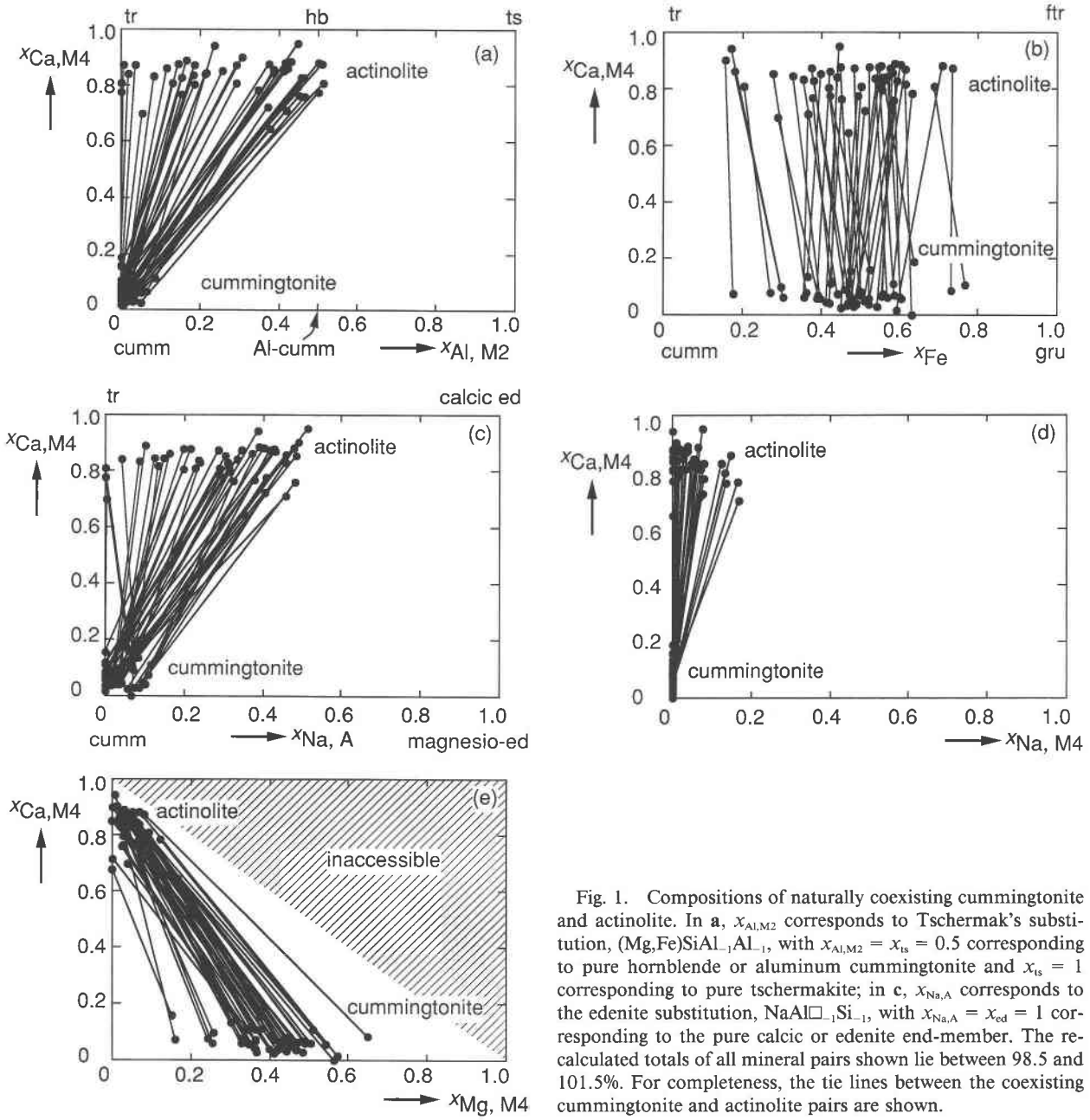

Fig. 1. Compositions of naturally coexisting cummingtonite and actinolite. In **a**, $x_{Al,M2}$ corresponds to Tschermak's substitution, (Mg,Fe)$SiAl_{-1}Al_{-1}$, with $x_{Al,M2} = x_{ts} = 0.5$ corresponding to pure hornblende or aluminum cummingtonite and $x_{ts} = 1$ corresponding to pure tschermakite; in **c**, $x_{Na,A}$ corresponds to the edenite substitution, $NaAl\square_{-1}Si_{-1}$, with $x_{Na,A} = x_{ed} = 1$ corresponding to the pure calcic or edenite end-member. The recalculated totals of all mineral pairs shown lie between 98.5 and 101.5%. For completeness, the tie lines between the coexisting cummingtonite and actinolite pairs are shown.

since, intuitively, large interaction parameters are expected to be associated with, for example, Tschermak and edenite substitutions. However, as indicated by the data, the interaction energies seem to counterbalance in the minerals analyzed, and macroscopically this justifies an ideal mixing description in the simple regions. With this, we may proceed to the extraction of the relevant DQF parameters from the data.

Description and extraction of the DQF parameters

For each simple region, the equilibrium relationships can be written in terms of mixing between real and fictive end-members. The real end-members are those whose compositions lie within the simple region; the fictive ones are those that lie outside the simple region and whose properties are chosen in such a way that the thermodynamic properties of the simple region are simple. In general, for a real end-member in a simple region,

$$\mu_i = G_i + RT \ln x_i + RT \ln \gamma_i$$

in which G_i is the (measureable) Gibbs energy of pure i, x_i is the thermodynamic mole fraction of i, and γ_i is the activity coefficient of i. For a fictive end-member in a simple region,

$$\mu_i' = G_i' + RT \ln x_i + RT \ln \gamma_i$$

in which G_i' is the Gibbs energy for the pure but fictive end-member i. In both expressions, the $RT \ln \gamma_i$ terms can be neglected because the amphibole data are consistent with ideal mixing in the simple regions (Fig. 1).

In considering the Gibbs energy of a fictive end-member, G_i', it is convenient when possible to express it in terms of a measured G_i, as $G_i' = G_i + I_i$, with the DQF term, I_i, corresponding to the difference in Gibbs energy between the real and the fictive end-member. In general, I_i may be expected to be temperature and pressure dependent, for example, $I_i = a + bT + cP$. The relationships for a complex binary system between the real G-x curves and a DQF description, including the relationship between G_i and G_i', are shown in Figure 3.

Using the above, the equilibria between coexisting cummingtonite and actinolite, Equation 1, can be considered. Assuming ideal mixing, the equilibrium condition becomes

$$\Delta\mu = 0 = \Delta G^0 + RT \ln K_{d(1)} \tag{2}$$

with the distribution coefficient known for each naturally coexisting mineral pair. From the way in which we defined our simple regions, the formulation of ΔG^0 involves real and fictive end-members for the equilibria (Eq. 1). For Equation 1, with k being cumm, the cummingtonite end-member is real in the mineral cummingtonite but fictive in actinolite, so using I values,

$$\begin{aligned}\Delta G^0 &= G_{\text{cumm}}^{\text{Act } C2/m} - G_{\text{cumm}}^{\text{Cumm } P2_1/m} \\ &= (G_{\text{cumm}}^{\text{Cumm } P2_1/m} + I_{\text{cumm}}^{\text{Act } C2/m}) - G_{\text{cumm}}^{\text{Cumm } P2_1/m} \\ &= I_{\text{cumm}}^{\text{Act } C2/m}\end{aligned} \tag{3}$$

where $G_{\text{cumm}}^{\text{Cumm } P2_1/m}$ is the Gibbs energy of pure end-member cummingtonite in the $P2_1/m$ structure of the real mineral cummingtonite and $G_{\text{cumm}}^{\text{Act } C2/m}$ is the Gibbs energy of the fictive $C2/m$ cummingtonite end-member in the mineral actinolite, with their difference corresponding to $I_{\text{cumm}}^{\text{Act } C2/m}$. Substituting Equation 3 into Equation 2 yields

$$-RT \ln K_{d(1)} = I_{\text{cumm}}^{\text{Act } C2/m}. \tag{4}$$

$I_{\text{cumm}}^{\text{Act } C2/m}$ is then found simply by substituting the thermodynamic mole fractions of $x_{\text{cumm}}^{\text{Cumm}}$ and $x_{\text{cumm}}^{\text{Act}}$ into the K_d term of Equation 4 for each mineral pair. This method can be followed for all the equilibria between the coexisting minerals in order to extract the DQF I parameters. The I term is the intercept of the horizontal line through the data with the $\ln K_d$ axis on the $\ln K_d - X_i$ diagrams in Figure 2.

Linear regression

Finding the I values is a linear regression problem and amounts to finding a best-fit estimate for the data, i.e., a solution for

$$y = X\Theta + e \tag{5}$$

with Θ the vector of the unknowns, e the vector of the error terms, and X and y the explanatory and response variables. The Θ and y are of length n and k, with k being the number of observations and n the number of unknowns. In general, the solution to Equation 5 is found as

$$\hat{\Theta} = (X^T V_y^{-1} X)^{-1} X^T V_y^{-1} y \tag{6}$$

(e.g., Mikhail, 1976) where V_y is the symmetric, k by k covariance matrix of y, with diagonal elements that are the squares of the standard deviation of the elements of y. The superscripts T and -1 denote transposed and inverse matrices, respectively.

In the case of interest here, there is only one variable, so $n = 1$, with X a unit column vector of length k, denoted 1. Hence, Equation 6 simplifies considerably and can be written as

$$\hat{\Theta} = \frac{1^T V_y^{-1} y}{1^T V_y^{-1} 1}.$$

This can be simplified further in the context of solving for the I's because our data are not correlated, so V_y is diagonal and

$$\hat{\Theta} = \frac{\sum_k \frac{y}{\sigma_{y_k}}}{\sum_k \frac{1}{\sigma_{y_k}}}.$$

The solution to such a one-dimensional problem can be found graphically by plotting the data on a diagram, with y/σ_y and $1/\sigma_y$ as vertical and horizontal axes, respectively; the slope of the best-fit line through the data and the origin is the required result, $\hat{\Theta}$. Finding a best-fit value for I from a knowledge of the compositions of coexisting amphibole pairs amounts to treating $\ln K_d$ as y and $\sigma(\ln K_d)$ as σ_y. Thus, $\hat{\Theta}$ is I/RT, with R being the gas constant. Since, in the first instance, we assume that the I's are independent of temperature and pressure, they are simply found by multiplying the slope of the best-fit line with the gas constant and a temperature that represents the conditions of formation of the original mineral pairs.

Having established the conceptual framework for finding a best-fit estimate for the DQF parameters, a regression estimator has to be chosen that is most appropriate for real data in order to solve Equation 5. The most commonly used regression method, least-squares (LS), involves finding a solution for which the sum of the squares of the residuals is minimized. LS gives optimum regressions of data (in a statistical sense) if the data to be analyzed are free of outliers; an outlier can be considered simply as a measurement that is discrepant with respect to the trend of the majority of the data. As soon as any data set contains outliers, LS techniques may give spurious results. Because of this, the classical estimator is usually inappropriate for real data (e.g., Rousseeuw and Leroy, 1987). Alternative statistical methods that can cope with outliers should be used to process data that may contain outliers. Statisticians call such methods "robust";

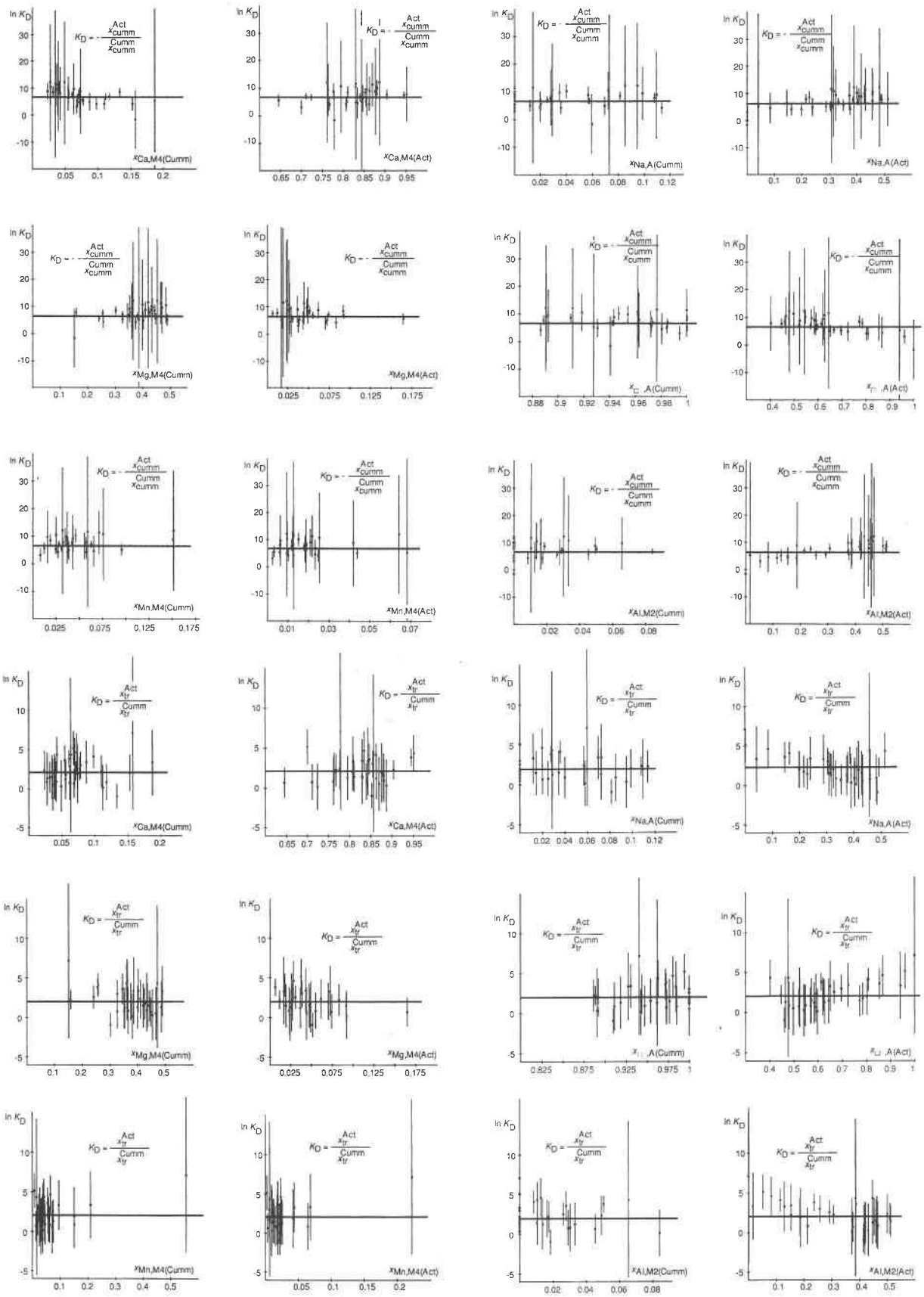
ln K_D
$K_D = \frac{Act}{Cumm}$
$x_{Ca,M4(Cumm)}$
$x_{Ca,M4(Act)}$
$x_{Na,A(Cumm)}$
$x_{Na,A(Act)}$
$x_{Mg,M4(Cumm)}$
$x_{Mg,M4(Act)}$
$x_{\square,A(Cumm)}$
$x_{\square,A(Act)}$
$x_{Mn,M4(Cumm)}$
$x_{Mn,M4(Act)}$
$x_{Al,M2(Cumm)}$
$x_{Al,M2(Act)}$
$x_{Ca,M4(Cumm)}$
$x_{Ca,M4(Act)}$
$x_{Na,A(Cumm)}$
$x_{Na,A(Act)}$
$x_{Mg,M4(Cumm)}$
$x_{Mg,M4(Act)}$
$x_{\square,A(Cumm)}$
$x_{\square,A(Act)}$
$x_{Mn,M4(Cumm)}$
$x_{Mn,M4(Act)}$
$x_{Al,M2(Cumm)}$
$x_{Al,M2(Act)}$

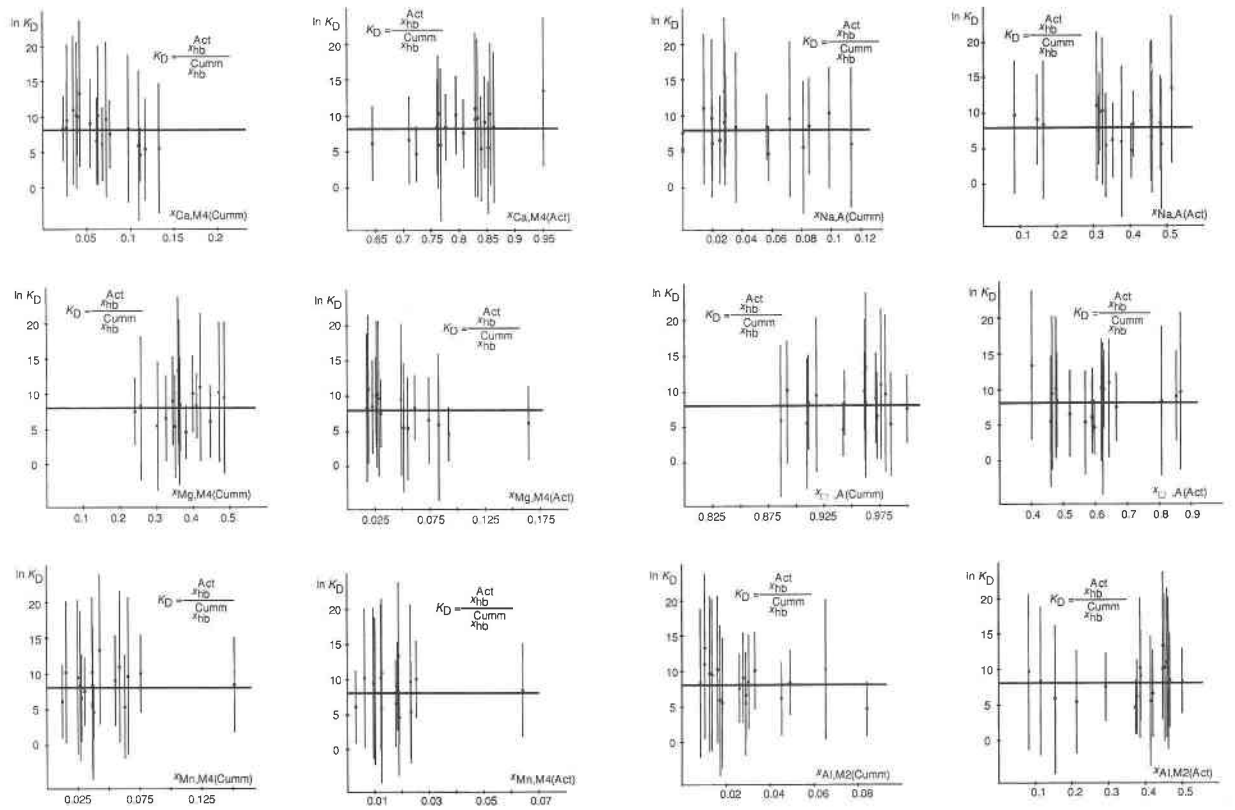

Fig. 2. Ln K_d vs. X_i diagrams corresponding to the equilibria of Equation 1. Within error, the data are fitted well by horizontal lines, demonstrating that the data are consistent with an ideal mixing description of the amphiboles in the simple regions. The error bars are 2σ. The ln K_d-axis intercept of the horizontal lines correspond to the I value. Note that these intercepts are constant for each equilibrium reaction.

they have been under development since the early 1960s (e.g., Huber, 1964) but have not yet been widely applied to geological problems. The regressions were undertaken using the least median of squares (LMS) estimator (Rousseeuw, 1984; Rousseeuw and Leroy, 1987). Graphically, the LMS estimator amounts to finding the minimum width band that covers 50% of the data. The band enables outliers to be identified, and once removed, a reweighted least-squares (RLS) solution can be obtained from the outlier-free data. An advantage of this combination of methods is that the uncertainty on the calculated I value comes as part of the RLS. A summary of this estimator and a geological application is given in Will and Powell (1991). A LMS/RLS program written in Mathematica (Wolfram, 1988) has been used to calculate the I values. As an example, Figure 4 shows the graphical output obtained from the program as part of the estimation of the I values. It has to be emphasized that despite our simplifying assumptions [i.e., ideal mixing and $I \neq f(P,T)$ in the simple regions] the fits of the data are remarkably good.

Results and an application

Using the approach outlined above, I values have been calculated for an independent set of end-members in the

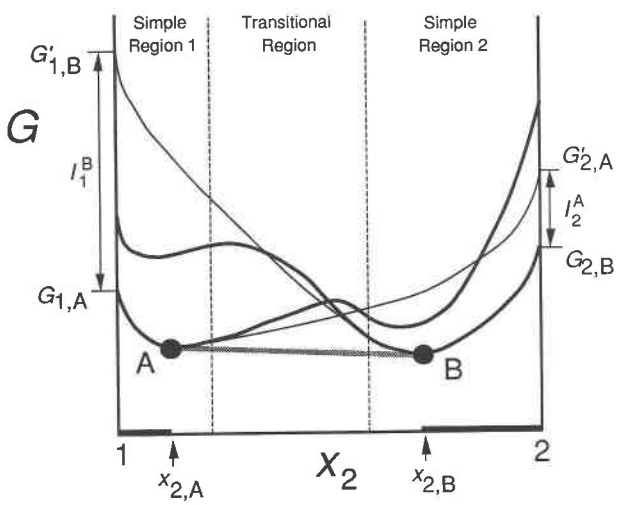

Fig. 3. G-x diagram illustrating the concept of real and fictive end-members in a binary system. Two phases, A and B, displaying nonideal mixing behavior (heavy lines) between end-members 1 and 2 are in equilibrium (shaded line). In each of the simple regions the mixing behavior of the solid solutions is modeled by an ideal mixing model (light lines). The difference in the Gibbs energy between a real and a fictive end-member is the term I.

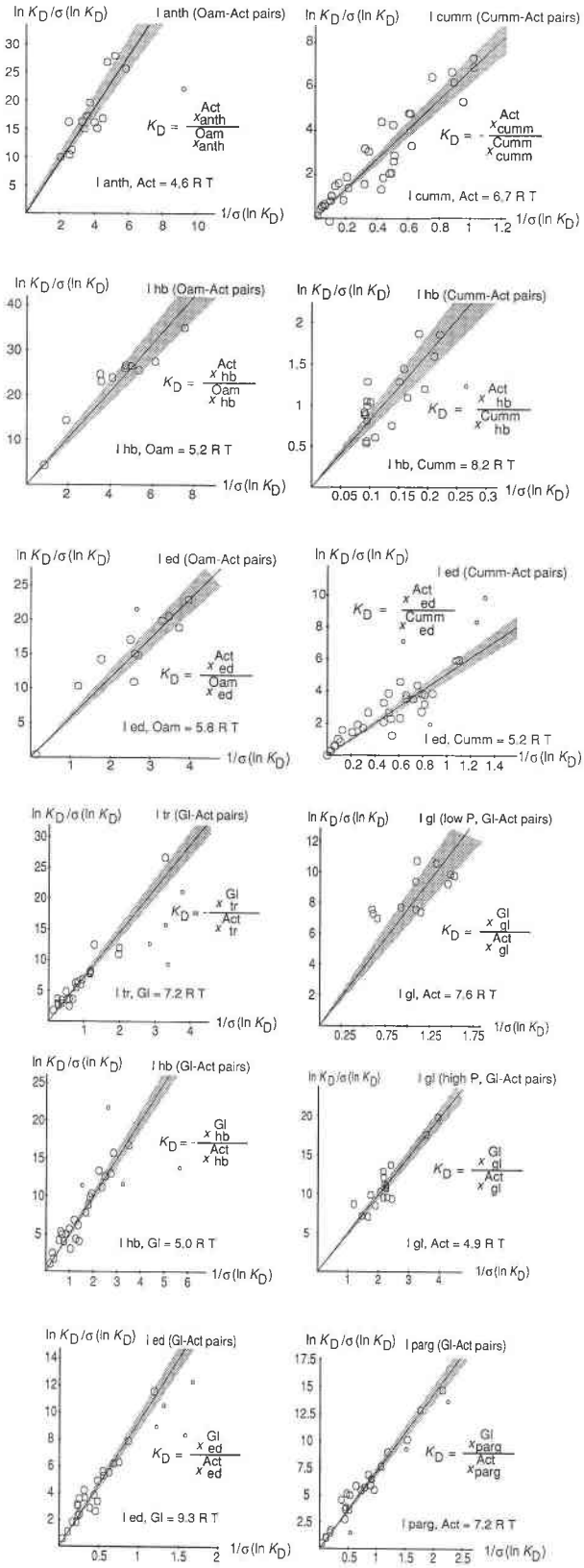

←

Fig. 4. Series of $\ln K_d/\sigma(\ln K_d)$ vs. $1/\sigma(\ln K_d)$ diagrams for coexisting amphiboles. Note that I_{gl}^{Act} has been estimated for different pressures of ≈8 kbar and ≈16 kbar, respectively. The shaded areas around the LMS/RLS best-fit line are the 95% confidence interval on the slope. The smaller circles are outliers as detected by LMS.

cummingtonite-actinolite, the calcic-sodic amphibole, and the anthophyllite-actinolite solid solutions. Amphibole chemical potentials involving I values can be summarized as follows, with the G_i provided, for example, by Holland and Powell (1990). (Units are in kJ/mol.) The I values and their 2σ uncertainties are grouped according to their reliability. The reliability levels are based on the number of amphibole pairs used to estimate the I values and are in sequence $1 > 2 > 3$.

1. For the cummingtonite-actinolite series (for T in the vicinity of 650 °C),

$$\mu^{Act}_{cumm} = G^{Cumm}_{cumm} + RT \ln x^{Act}_{cumm} + 51.5\ (\pm 4.5)$$

$$\mu^{Cumm}_{tr} = G^{Act}_{tr} + RT \ln x^{Cumm}_{tr} + 16.0\ (\pm 3.8)$$

$$\mu^{Cumm}_{hb} = G^{Act}_{hb} + RT \ln x^{Cumm}_{hb} + 62.6\ (\pm 8.6)$$

$$\mu^{Cumm}_{ed} = G^{Act}_{ed} + RT \ln x^{Cumm}_{ed} + 40.1\ (\pm 3.7)$$

$$\mu^{Cumm}_{parg} = G^{Act}_{parg} + RT \ln x^{Cumm}_{parg} + 12.6\ (\pm 1.3).$$

2. For the calcic-sodic amphibole series (for T in the vicinity of 500 °C),

$$\mu^{Act}_{gl} = G^{Gl}_{gl} + RT \ln x^{Act}_{gl} + 48.7\ (\pm 6.7)\ \text{(low } P\text{)}$$

$$\mu^{Act}_{gl} = G^{Gl}_{gl} + RT \ln x^{Act}_{gl} + 31.8\ (\pm 2.9)\ \text{(high } P\text{)}$$

$$\mu^{Act}_{rich} = G^{Gl}_{rich} + RT \ln x^{Act}_{rich} + 25.0\ (\pm 3.0)$$

$$\mu^{Gl}_{tr} = G^{Act}_{tr} + RT \ln x^{Gl}_{tr} + 46.3\ (\pm 3.4)$$

$$\mu^{Gl}_{hb} = G^{Act}_{hb} + RT \ln x^{Gl}_{hb} + 32.1\ (\pm 2.0)$$

$$\mu^{Gl}_{ed} = G^{Act}_{ed} + RT \ln x^{Gl}_{ed} + 59.8\ (\pm 3.8)$$

$$\mu^{Gl}_{parg} = G^{Act}_{parg} + RT \ln x^{Gl}_{parg} + 46.0\ (\pm 2.5).$$

3. For the orthoamphibole-actinolite series (for T in the vicinity of 650 °C),

$$\mu^{Act}_{anth} = G^{Oam}_{anth} + RT \ln x^{Act}_{anth} + 35.4\ (\pm 4.0)$$

$$\mu^{Oam}_{tr} = G^{Act}_{tr} + RT \ln x^{Oam}_{tr} + 34.5\ (\pm 6.5)$$

$$\mu^{Oam}_{hb} = G^{Act}_{hb} + RT \ln x^{Oam}_{hb} + 40.1\ (\pm 4.8)$$

$$\mu^{Oam}_{ed} = G^{Act}_{ed} + RT \ln x^{Oam}_{ed} + 44.3\ (\pm 4.1)$$

$$\mu^{Oam}_{parg} = G^{Act}_{parg} + RT \ln x^{Oam}_{parg} + 54.5\ (\pm 4.4).$$

The low- and high-pressure values for μ^{Act}_{gl} correspond to pressures of some 8 and 16 kbar, respectively. Alternatively, $\mu^{Act}_{gl} = 65.6 - 2.1P$ (kbar).

These are the chemical potentials for independent sets of amphibole end-members; the chemical potentials for dependent amphibole end-members can be found by linear combination. For example, orthoamphiboles in cordierite + orthoamphibole assemblages from the Springton area in South Australia are extremely rich in the edenite end-member, with $NaAl^{[4]}\square_{-1}Si_{-1}$ up to 0.7 (Arnold and Sandiford, 1990). Thus, for an ortho-edenite, $NaMg_2Mg_3Mg_2(Si_3Al)Si_4O_{22}(OH)_2$, in orthoamphibole, the chemical potential is obtained by a linear combination of those of the edenite, anthophyllite, and tremolite end-members in the orthorhombic *Pnma* structure:

$$\begin{aligned}\mu_{oed}^{Oam} &= \mu_{ed}^{Oam} + \mu_{anth}^{Oam} - \mu_{tr}^{Oam} \\ &= (G_{ed}^{Act} + RT \ln x_{cd}^{Oam} + 44.3) \\ &\quad + (G_{anth}^{Oam} + RT \ln x_{anth}^{Oam}) \\ &\quad - (G_{tr}^{Act} + RT \ln x_{tr}^{Oam} + 34.5) \\ &= G_{ed}^{Act} + G_{anth}^{Oam} - G_{tr}^{Act} + RT \ln x_{oed}^{Oam} + 9.8.\end{aligned}$$

The application of these DQF results will be illustrated with an example.

The cummingtonite component in tremolite

Experimental studies in the system CaO-MgO-SiO_2-H_2O (CMSH) by Jenkins (1987) and Pawley (cited in Graham et al., 1989), conducted over a wide range of pressures and temperatures, indicate that pure tremolite cannot be synthesized from starting materials with bulk compositions of pure tremolite or even from mixtures with a Ca/Mg ratio greater than 2/5. Instead, at the conditions of synthesis, both studies showed that the stable amphibole contains a small but significant amount of the cummingtonite end-member. At 6 kbar and 850 °C, the stable amphibole composition approximates $tr_{90}cumm_{10}$, i.e., $x_{Ca,M4} = 0.9 \pm 0.03$ (Jenkins, 1987). In both studies, the stable mineral assemblage at these conditions was found to be amphibole + quartz in the absence of clino- and orthopyroxene. Jenkins (1987) observed that the assemblage amphibole + quartz coexisted with clinopyroxene if the amphibole was more calcic than $x_{Ca,M4} = 0.90$, whereas for $x_{Ca,M4} < 0.90$ this assemblage coexisted stably with orthopyroxene. This effect of the $CaMg_{-1}$ substitution on the M4 site in amphiboles has not only been documented for synthetic amphiboles but is also a common feature in naturally occurring amphiboles (Jenkins, 1987, and references therein).

Using the results of our DQF approach, particularly I_{cumm}^{Act} and I_{tr}^{Cumm}, the amphibole compositions in the CMSH equilibria described above have been calculated at the conditions of concern. At 6 kbar and 850 °C with H_2O in excess, the CMSH divariant assemblage amph + cpx + q (+ H_2O) is stable for $x_{Ca,M4}$ in amphibole >0.92, whereas amph + opx + q (+ H_2O) is stable for $x_{Ca,M4} < 0.86$. The CMSH trivariant assemblage amph + q (+ H_2O) is only stable for $0.86 < x_{Ca,M4} < 0.92$ (Fig. 5). This is in excellent agreement with the compositional range of 0.9 ± 0.03 for $x_{Ca,M4}$ found by Jenkins (1987).

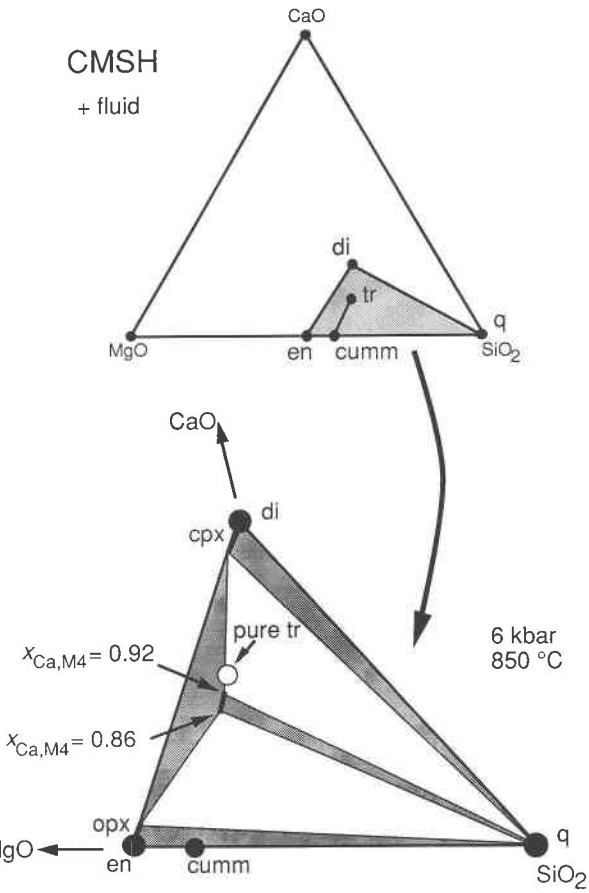

Fig. 5. Position of the pure end-member compositions (dots) of the phases involved in the CMSH tremolite breakdown reaction 2tr = 3en + 4di + 2q + $2H_2O$. Note that there is a solid solution between diopside and enstatite as well as between tremolite and cummingtonite (**top**). Enlargement of shaded area (**bottom**): At 6 kbar and 850 °C the assemblage cpx-q coexists with amphiboles more calcic than $x_{Ca,M4} = 0.92$; the assemblage opx-q with amphiboles less calcic than $x_{Ca,M4} = 0.86$. Only amphiboles with compositions intermediate to those two occur stably with quartz without pyroxene. Note that there is a limited $CaMg_{-1}$ substitution in clinopyroxenes (cpx) away from the pure diopside end-member and also a very small $MgCa_{-1}$ substitution in orthopyroxenes (opx) away from the pure enstatite end-member.

Both experimental work and studies on natural amphiboles (Cameron, 1975; Robinson et al., 1982; Jenkins, 1987) suggest that $x_{Ca,M4}$ in tremolite decreases with an increase in temperature. Our calculated amphibole compositions along the cummingtonite-tremolite join agree with this observation. The T-$x_{Ca,M4}$ projection (Fig. 6a) shows the change in $x_{Ca,M4}$ in amphiboles, as calculated by applying the DQF results, along the CMSH amphibole breakdown reaction, tr = di + en + q + H_2O (Fig. 6b). In Figure 6a the compositions of the two pyroxenes have been omitted for clarity. Figure 6a suggests strongly that

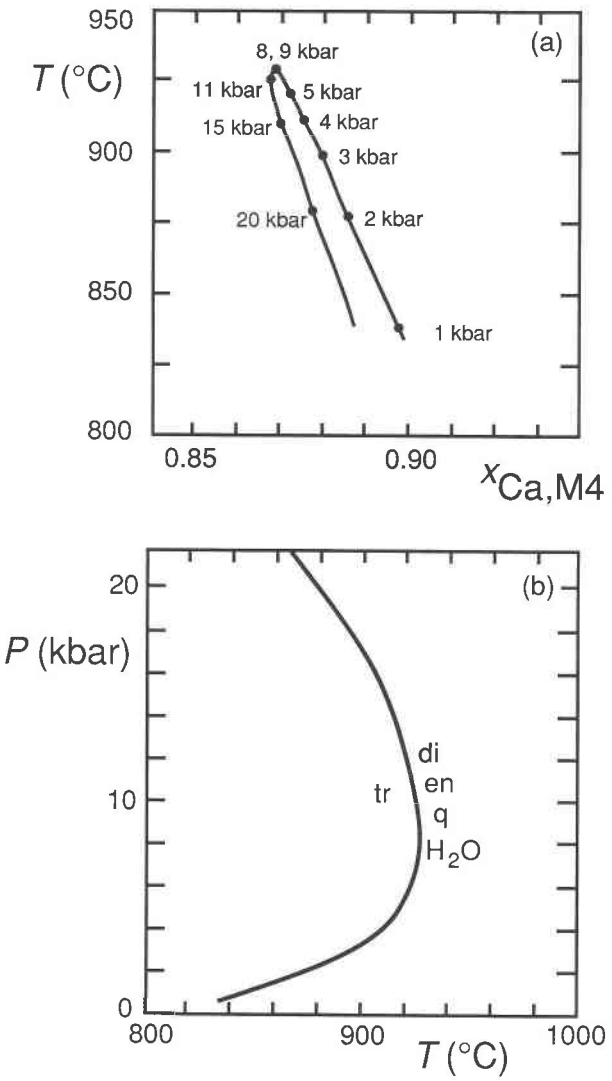

Fig. 6. (**a**) Calculated compositional change of tremolite with temperature along the CMSH univariant reaction tr = di + en + q + H_2O. The T-x_{Ca} relationship seems to indicate that there is an inverse relationship between temperature and the cummingtonite component in tremolite. (**b**) Upper thermal stability limit of the amphibole involved in the breakdown reaction in P-T space.

there is an inverse relationship between temperature and $x_{Ca,M4}$ in amphiboles in this equilibrium assemblage. The $x_{Ca,M4}$ contents decrease with increasing temperature until this dehydration reaction reaches its maximum temperature at some 8–9 kbar. At pressures higher than this maximum, the $x_{Ca,M4}$ contents increase with decreasing temperatures. This behavior matches exactly the one proposed by Jenkins (1987). Note that along this reaction curve, both orthopyroxene andd clinopyroxene are also subject to $CaMg_{-1}$ substitutions. The calculated sequence is $x_{Ca,cpx} > x_{Ca,amph} > x_{Ca,opx}$. The inverse relationship between temperature and x_{Ca} is also true for the two pyroxenes.

Discussion and conclusion

Coexisting phases have been used in the past to constrain the thermodynamic properties of minerals (e.g., Wood and Banno, 1973; Perchuk et al., 1981). In fact Wood and Banno's (1973) approach to orthopyroxene + clinopyroxene equilibria closely parallels our work here in that they used an ideal mixing model and put all nonideality into the standard state properties (I in our terminology). In a more sophisticated approach and with much more data on coexisting amphiboles than are currently available, nonzero interaction parameters, w_{ij}, and a pressure and temperature dependence of the I terms will need to be introduced. Because interaction parameter and I terms are correlated, the I required will vary, depending on the choice of, and magnitude of, the interaction parameters. For a particular set of coexisting amphiboles (or pyroxenes, etc.), the $RT \ln \gamma$ combined with the I value will be strongly correlated.

The DQF model describes the observed mineral equilibria remarkably well. Our DQF data should yield satisfactory results in calculations as long as they are applied in the same compositional and temperature range as the original mineral data from which the DQF data were extracted (i.e., amphibolite facies for cummingtonite-actinolite and orthoamphibole-actinolite solid solutions and greenschist-blueschist and eclogite facies for the actinolite-glaucophane solid solution). Extrapolation to compositions or temperature conditions not covered by our data is not advised. Extension of this coverage awaits the publication of natural mineral data that are outside the composition and temperature ranges covered here (please send us your unpublished mineral data on coexisting amphiboles). Nevertheless, the amphibole thermodynamic parameters presented here cover most of the greenschist-blueschist facies transition and amphibolite facies equilibria relevant to amphibole-bearing assemblages and allow the calculation of equilibria containing coexisting amphiboles (e.g., actinolite + glaucophane involved in greenschist-blueschist facies transition equilibria) for the first time.

References cited

Arnold, J., and Sandiford, M. (1990) Petrogenesis of cordierite-orthoamphibole assemblages from the Springton region, South Australia. Contributions to Mineralogy and Petrology, 106, 100–109.

Brady, J.B. (1974) Coexisting actinolite and hornblende from west-central New Hampshire. American Mineralogist, 59, 529–535.

Cameron, K.L. (1975) An experimental study of actinolite-cummingtonite phase relations with notes on the synthesis of Fe-rich anthophyllite. American Mineralogist, 60, 375–390.

Darken, L.S. (1967) Thermodynamics of binary metallic solutions. Transactions of the Metallurgical Society of AIME, 239, 80–89.

Das Gupta, S.P. (1972) Coexisting hornblende and cummingtonite from the Khetri copper belt, Rajasthan, India. Mineralogical Magazine, 38, 890–893.

Ernst, W.G., and Dal Piaz, G.V. (1978) Mineral parageneses of eclogitic rocks and related mafic schists of the Piemonte ophiolite nappe, Breuil–St. Jacques area, western Italian Alps. American Mineralogist, 63, 621–640.

Ernst, W.G., Seki, Y., Onuki, H., and Gilbert, M.C. (1970) Comparative

study of low-grade metamorphism in the California coast ranges and the outer metamorphic belt of Japan. Geological Society of America Memoir, 124, 276 p.

Ghose, S. (1981) Subsolidus reactions and microstructures in amphiboles. In Mineralogical Society of America Reviews in Mineralogy, 9A, 325–372.

Graham, C.M., Maresch, W.V., Welch, M.D., and Pawley, A.R. (1989) Experimental studies on amphiboles: A review with thermodynamic perspectives. European Journal of Mineralogy, 1, 535–555.

Haslam, H.W., and Walker, B.G. (1971) A metamorphosed pyroxenite at Nero Hill, Central Tanzania. Mineralogical Magazine, 38, 58–63.

Hawthorne, F.C., and Griep, J.L. (1980) A three amphibole assemblage from the Tallan Lake Sill, Peterborough County, Ontario. Canadian Mineralogist, 18, 275–284.

Himmelberg, G.R., and Papike, J.J. (1969) Coexisting amphiboles from blueschist facies metamorphic rocks. Journal of Petrology, 10, 102–114.

Holland, T.J.B., and Powell, R. (1990) An enlarged and updated internally consistent thermodynamic dataset with uncertainties and correlations: The system K_2O-Na_2O-CaO-MgO-MnO-FeO-Fe_2O_3-Al_2O_3-TiO_2-SiO_2-C-H_2-O_2. Journal of Metamorphic Geology, 8, 89–124.

Huber, P.J. (1964) Robust estimation of a local parameter. Annals of Mathematical Statistics, 35, 73–101.

Immega, I.P., and Klein, C. (1976) Mineralogy and petrology of some metamorphic Precambrian iron formations in southwestern Montana. American Mineralogist, 61, 1117–1144.

James, R.S., Grieve, R.A.F., and Pand, L. (1978) The petrology of cordierite-anthophyllite gneisses and associated mafic and pelitic gneisses at Manitouwadge, Ontario. American Journal of Science, 278, 41–63.

Jenkins, D.M. (1987) Synthesis and characterization of tremolite in the system H_2O-CaO-MgO-SiO_2. American Mineralogist, 72, 707–715.

Kisch, H.J. (1969) Magnesiocummingtonite-$P2_1/m$: A Ca- and Mn-poor clino-amphibole from New South Wales. Contributions to Mineralogy and Petrology, 21, 319–331.

Kisch, H.J., and Warnaars, F.W. (1969) Distribution of Mg and Fe in cummingtonite-hornblende and cummingtonite-actinolite pairs from metamorphic assemblages. Contributions to Mineralogy and Petrology, 24, 245–267.

Klein, C. (1968) Coexisting amphiboles. Journal of Petrology, 9, 281–330.

——— (1969) Two-amphibole assemblages in the system actinolite-hornblende-glaucophane. American Mineralogist, 54, 212–237.

Mikhail, E.M. (1976) Observations and least squares. IEP-Dun Donnelley, New York.

Perchuk, L.L., Podlesskii, K.K., and Aranovich, L.Ya. (1981) Calculation of thermodynamic properties of end-member minerals from natural parageneses. In R.C. Newton, A. Navrotsky, and B.J. Wood, Eds., Advances in physical geochemistry, vol. 1, Thermodynamics of minerals and melts, p. 111–129. Springer, New York.

Powell, R. (1987) Darken's quadratic formalism and thermodynamics of minerals. American Mineralogist, 72, 1–11.

Reynard, B., and Ballèvre, M. (1988) Coexisting amphiboles in an eclogite from the western Alps: New constraints on the miscibility gap between sodic and calcic amphiboles. Journal of Metamorphic Geology, 6, 333–350.

Robinson, P., Spear, F.S., Schumacher, J.C., Laird, J., Klein, C., Ewans, B.W., and Doolan, B.L. (1982) Phase relations of metamorphic amphiboles: Natural occurrence and theory. In Mineralogical Society of America Reviews in Mineralogy, 9B, 1–227.

Rousseeuw, P.J. (1984) Least median of squares regression. Journal of the American Statistical Association, 59, 871–880.

Rousseeuw, P.J., and Leroy, A.M. (1987) Robust regression and outlier detection. Wiley, New York.

Sampson, G.A., and Fawcett, J.J. (1977) Coexisting amphiboles from the Hastings region of southeast Ontario. Canadian Mineralogist, 15, 283–296.

Schliestedt, M. (1986) Eclogite-blueschist relationships as evidenced by mineral equilibria in the high-pressure metabasic rocks of Sifnos (Cycladic Islands), Greece. Journal of Petrology, 27, 1437–1459.

Smelik, E.A., Nyman, M.W., and Veblen, D.R. (1991) Pervasive exsolution within the calcic amphibole series: TEM evidence for a miscibility gap between actinolite and hornblende in natural samples. American Mineralogist, 76, 1184–1204.

Stephenson, N.C.N., and Hensel, H.D. (1979) Intergrown calcic and Fe-Mg amphiboles from the Wongwibinda metamorphic complex, N.S.W., Australia. Canadian Mineralogist, 17, 11–23.

Triboulet, C. (1978) Coexisting blue and blue-green amphiboles from Ile de Groix (Moribihan, France). Journal of Petrology, 19, 653–668.

Will, T.M., and Powell, R. (1991) A robust approach to the calculation of paleostress fields from fault plane data. Journal of Structural Geology, 13, 813–821.

Wolfram, S. (1988) Mathematica. A system for doing mathematics by computer. Addison-Wesley, Redwood City, California.

Wood, B.J., and Banno, S. (1973) Garnet-orthopyroxene and orthopyroxene-clinopyroxene relationships in simple and complex systems. Contributions to Mineralogy and Petrology, 42, 109–124.

Manuscript received February 8, 1991
Manuscript accepted April 28, 1992

Appendix 1. Error propagation

The general form of the error propagation equation for a vector of linear functions, $y = f(x)$, is

$$V_y = JV_xJ^T \tag{A1}$$

(Mikhail, 1976) with V_x and V_y the covariance matrices of x and y, and with J, the Jacobian, containing the partial derivatives of y with respect to x. The superscript T denotes a transposed matrix. If y is a scalar and V_x is diagonal, then Equation A1 simplifies to

$$\sigma_y^2 = \sum_i \left(\frac{\partial y}{\partial x_i}\right)^2 \sigma_{x_i}^2.$$

This latter equation can be used to give the standard deviation on $\ln K_d$, $\sigma(\ln K_d)$, for end-member j in, for example, coexisting cummingtonite-actinolite:

$$\sigma(\ln K_d)^2 = \left(\frac{\sigma_{x_j\text{-cumm}}}{x_{j\text{-cumm}}}\right)^2 + \left(\frac{\sigma_{x_j\text{-act}}}{x_{j\text{-act}}}\right)^2.$$

The uncertainties on the thermodynamic mole fractions come from the analytical uncertainties and from the assignment of total Fe as FeO into FeO and Fe_2O_3. The standard deviations on the weight percent of the oxides, w_i, are taken to follow the relationship $\sigma_{w_i} = 0.01w_i + 0.05$.

The uncertainty on the mole fraction of the end-members j is given by

$$\sigma_{x_j}^2 = \sum_i \left(\frac{\partial x_j}{\partial w_i}\right)\sigma_{w_i}^2 + 2\left(\frac{\partial x_j}{\partial w_{\text{FeO}}}\right)\left(\frac{\partial x_j}{\partial w_{\text{Fe}_2\text{O}_3}}\right)\sigma_{w_{\text{FeO}}w_{\text{Fe}_2\text{O}_3}} \tag{A2}$$

with i being over the oxides. The partial derivatives in the first sum were determined by finite difference. The last term arises because the calculated w_{FeO} and $w_{\text{Fe}_2\text{O}_3}$ derived from the total Fe as FeO, w_{FeO}^0, are correlated. The covariance can be derived using Equation A2 as follows:

$$y = \begin{bmatrix} w_{\text{FeO}} \\ w_{\text{Fe}_2\text{O}_3} \end{bmatrix}$$

and

$$x = \begin{bmatrix} w^0_{FeO} \\ p \end{bmatrix}$$

in which p is the proportion of total Fe as FeO to be converted to Fe_2O_3. For the distribution of Fe^{2+} and Fe^{3+}, the system of linear equations is given by

$$w_{FeO} = (1 - p)w^0_{FeO}$$

and

$$w_{Fe_2O_3} = \text{fac}\ p w^0_{FeO}$$

with fac = molecular weight(Fe_2O_3)/[2 molecular weight (FeO)] ≅ 1.1113. The Jacobian, J, is

$$J = \begin{bmatrix} \frac{\partial w_{FeO}}{\partial w^0_{FeO}} & \frac{\partial w_{FeO}}{\partial p} \\ \frac{\partial w_{Fe_2O_3}}{\partial w^0_{FeO}} & \frac{\partial w_{Fe_2O_3}}{\partial p} \end{bmatrix} = \begin{bmatrix} (1 - p) & -w^0_{FeO} \\ \text{fac}\ p & \text{fac}\ w^0_{FeO} \end{bmatrix}.$$

The covariance matrix for x is

$$V_x = \begin{bmatrix} \sigma^2_{w^0_{FeO}} & 0 \\ 0 & \sigma^2_{w_p} \end{bmatrix}.$$

The off-diagonal elements of V_x are zero because w^0_{FeO} and p are uncorrelated. The covariance matrix for y, V_y, is symmetric and has the following form:

$$V_y = \begin{bmatrix} \sigma^2_{w^0_{FeO}} & \sigma^2_{w_{FeO}w_{Fe_2O_3}} \\ \sigma_{w_{FeO}w_{Fe_2O_3}} & \sigma^2_{w_{Fe_2O_3}} \end{bmatrix}$$

in which $\sigma_{w_{FeO}}$ and $\sigma_{w_{Fe_2O_3}}$ are the standard deviations on w_{FeO} and $w_{Fe_2O_3}$ and the off-diagonal covariance term describes the mutual variation of these two variables. Substituting into Equation A1 and multiplying out yields

$$\sigma^2_{w_{FeO}} = (1 - p)^2\sigma^2_{w^0_{FeO}} + (w^0_{FeO})^2\sigma^2_p$$
$$\sigma^2_{w_{Fe_2O_3}} = \text{fac}^2[p^2\sigma^2_{w^0_{FeO}} + (w^0_{FeO})^2\sigma^2_p]$$
$$\sigma_{w_{FeO}w_{Fe_2O_3}} = \text{fac}[p(1 - p)\sigma^2_{w^0_{FeO}} - (w^0_{FeO})^2\sigma^2_p].$$

These are substituted into Equation A2 with $\sigma_p = 0.1$ as a suitably large uncertainty on the proportion of FeO converted to Fe_2O_3.